J|A|C|S COMMUNICATIONS

Published on Web 01/02/2009

Photoassisted Overall Water Splitting in a Visible Light-Absorbing Dye-Sensitized Photoelectrochemical Cell

W. Justin Youngblood,[†] Seung-Hyun Anna Lee,[†] Yoji Kobayashi,[†] Emil A. Hernandez-Pagan,[†] Paul G. Hoertz,[†] Thomas A. Moore,[‡] Ana L. Moore,[‡] Devens Gust,[‡] and Thomas E. Mallouk*,[†]

Department of Chemistry, The Pennsylvania State University, University Park, Pennsylvania 16802, and Department of Chemistry and Biochemistry, Arizona State University, Tempe, Arizona 85287

Received November 20, 2008; E-mail: tom@chem.psu.edu

Photocatalytic water splitting uses light energy to drive the thermodynamically uphill conversion of water into its constituent elements. Fujishima and Honda reported the first example of overall water splitting with TiO_2 photoelectrodes under UV illumination in 1972,[1] and more efficient multijunction photoelectrodes have subsequently been reported.[2,3] More recently, Maeda et al. have developed a photocatalytic water splitting system based on oxynitride semiconductor particles.[4] In comparison, progress on overall water splitting in molecular photosystems systems has been slow. The use of sacrificial oxidizing and reducing agents has enabled separate explorations of the hydrogen- and oxygen-evolving half-reactions.[5,6] However, despite recent progress on water oxidation catalysts,[7−12] the rate of hole scavenging is in general too slow to compete with back electron transfer in artificial photosynthetic systems.

Hydrated iridium oxide ($IrO_2 \cdot nH_2O$) was first characterized as an effective water oxidation catalyst by Harriman et al.[13] Water oxidation can be driven with this catalyst using photochemically generated Ru(III) tris(bipyridine). We previously reported optimized conditions for this regenerative system.[14] Recently, we found that the size and polydispersity of colloidal $IrO_2 \cdot nH_2O$ particles could be controlled by using bidentate carboxylic acid stabilizers.[15] This strategy resulted in small (1−5 nm), well-dispersed particles rather than the larger (10−30 nm), aggregated colloids that are produced by using citric acid as a stabilizer. Ruthenium polypyridyl dyes modified with bidentate carboxylates can serve as effective stabilizers for these clusters. The rate of electron transfer for such chemisorbed dyes on $IrO_2 \cdot nH_2O$ is in the range of 10^3 s^{-1}, significantly faster than it is for unbound dyes in the presence of $IrO_2 \cdot nH_2O$ colloids.

We designed the heteroleptic ruthenium dye **1** to serve as both a sensitizer component and a molecular bridge to connect $IrO_2 \cdot nH_2O$ particles to a metal oxide semiconductor. Phosphonates are chemically selective for TiO_2 and the malonate group is selective for $IrO_2 \cdot nH_2O$. The bpy ligands in this complex minimize the distance between the ruthenium center and the surfaces of the respective oxides. The synthetic procedures for these ligands and their incorporation into dye **1** were based on literature precedents (see Supporting Information).

Dye **1** serves as an effective stabilizer for $IrO_2 \cdot nH_2O$, producing well-dispersed particles of ∼2 nm diameter (Figure S1). Upon pulsed laser excitation (532 nm, 15 ns) of this photosensitized colloid in a 1 M solution of $Na_2S_2O_8$, electron transfer from the excited-state of **1** to $S_2O_8^{2-}$ is followed by electron transfer from the particles to the photo-oxidized dye with a first-order lifetime

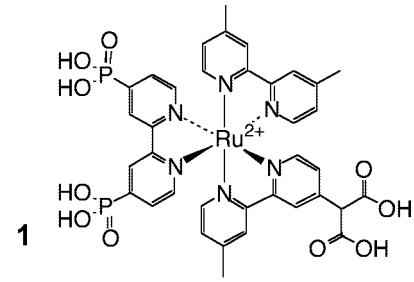

of 2.2 ms (Figure 1). The bleaching recovery reaction is not 100% complete on the time scale shown in Figure 1, consistent with some other irreversible process (photo-oxidation or desorption of the dye) that competes with electron transfer from $IrO_2 \cdot nH_2O$. Without $S_2O_8^{2-}$ in the solution, the luminescence of **1** (whose unperturbed excited-state lifetime is 0.30 μs at pH 5.8) is instead quenched within ∼30 ns by the $IrO_2 \cdot nH_2O$ particles. These kinetics are summarized in Figure 1.

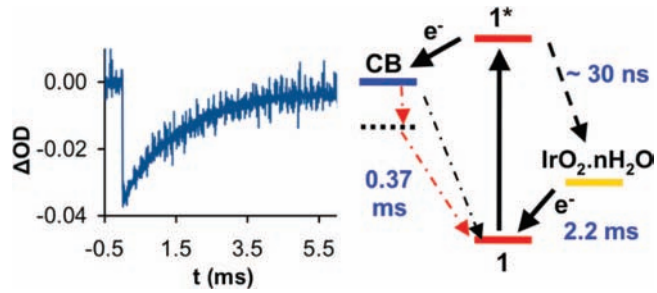

Figure 1. (Left) Bleaching recovery trace (470 nm) for sensitizer **1** adsorbed on $IrO_2 \cdot nH_2O$ nanoparticles in aqueous $S_2O_8^{2-}$ solution. Excitation source: 15 ns Nd:YAG laser, 532 nm. (Right) Measured time constants for forward and back electron transfer reactions of **1**-stabilized $IrO_2 \cdot nH_2O$ nanoparticles adsorbed on a TiO_2 nanoparticle film. CB = conduction band. Dashed line represents trap states below the CB edge.

When the dye-$IrO_2 \cdot nH_2O$ colloid was adsorbed onto nanoparticulate anatase TiO_2, we observed rapid electron injection into the oxide semiconductor, followed by back electron transfer (∼0.37 ms, Figure S3). This back transfer from TiO_2 (CB) to the oxidized dye is an order of magnitude faster than the forward electron transfer from $IrO_2 \cdot nH_2O$ to the oxidized dye.

We made photoelectrochemical cells in an H-configuration, containing a working electrode composed of a porous nanocrystalline TiO_2 film (1 cm^2 area, 9 μm thickness) on F-SnO_2 and sensitized with the dye-$IrO_2 \cdot nH_2O$ colloid. The architecture of the dye-sensitized anode is shown schematically in Figure 2. A Pt wire counter electrode and Ag/AgCl reference electrode were separated

[†] The Pennsylvania State University.
[‡] Arizona State University.

10.1021/ja809108y CCC: $40.75

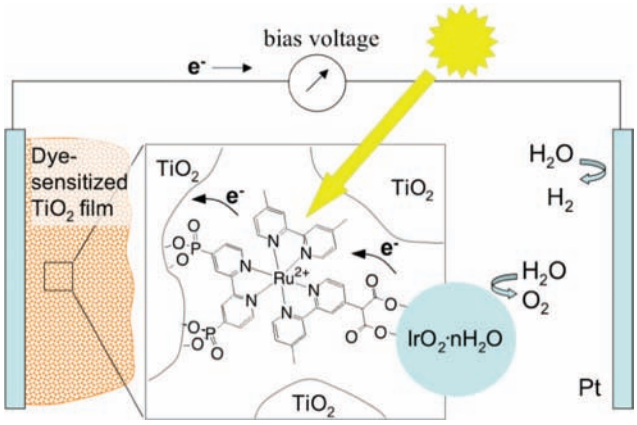

Figure 2. Schematic of the water splitting dye sensitized solar cell.

from the working electrode by a coarse glass frit, and the three electrodes were immersed in a solution of 30 mM Na_2SiF_6 (buffered to pH 5.75 with $NaHCO_3$) and 500 mM Na_2SO_4. Irradiation of the working electrode with visible light ($\lambda > 410$ nm) at potentials positive of −325 mV vs Ag/AgCl produced a measurable photoanodic current (Figure 3). As the cell was connected at each applied

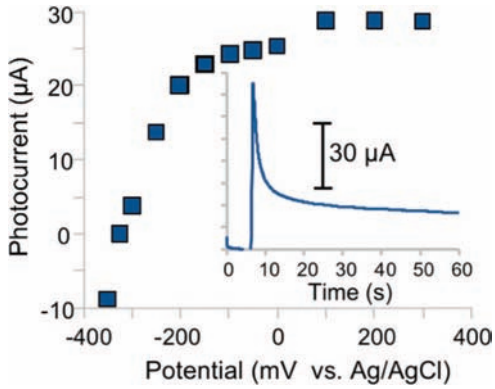

Figure 3. Steady-state photocurrent vs anode potential. Inset shows a photocurrent transient recorded at 0 mV vs Ag/AgCl/saturated NaCl.

potential, there was an anodic current spike that decayed rapidly followed by a steady current (typically 10−30 μA, Figure 3). Under steady illumination, the current decayed over a period of ∼4 h. In comparison, an identical cell with an unsensitized TiO_2 film electrode gave a steady photocurrent of only 1−2 μA.

In the configuration shown in Figure 2, the dye-$IrO_2 \cdot nH_2O$ colloid replaces the visible light-absorbing sensitizer of a dye-sensitized solar cell (DSSC),[16] and water replaces iodide as the electron donor. Another way to describe this photoelectrochemical cell is as a dye-sensitized version of the Fujishima−Honda cell.[1] As in the Fujishima−Honda cell, a small applied bias is needed to achieve overall water splitting, because electrons in trap states below the TiO_2 conduction band edge are not sufficiently reducing to generate hydrogen and rapidly recombine. To achieve overall water splitting without an applied bias in this system, one would need to use a semiconductor with a more negative conduction band edge potential and/or significantly reduce the recombination rate of trapped electrons. However, preliminary transient spectroscopy with dye-sensitized mesoporous films of Nb_2O_5 shows that back electron transfer from Nb_2O_5 is even faster than from TiO_2 with dye **1**.

Using 450 nm light at 7.8 mW/cm^2 intensity, we measured 12.7 μA/cm^2 photocurrent from a sensitized working electrode with $A_{464} = 0.67$, corresponding to an internal quantum yield of ∼0.9%. Measurements of plateau photocurrent as a function of applied bias (Figure 3) gave an open circuit potential of −325 mV vs Ag/AgCl. From the formal potential of the oxygen-water couple at this pH (+650 mV), we obtain an open circuit photovoltage of 0.98 V. The formation of oxygen and hydrogen at the anode and cathode of the cell was confirmed by gas chromatography. The oxygen yield was also measured by using a pseudo-Clark electrode in the anode compartment of the cell (see Supporting Information). Under these conditions, the current efficiency for photoanodic oxygen generation was roughly 20%.

The decay in photocurrent of the sensitized working electrode was always accompanied by bleaching of the visible absorbance of the film. This is likely due to nucleophilic attack on the oxidized dye, a reaction that is known to compete with water oxidation in sacrificial photosystems that incorporate $[Ru(bpy)_3]^{2+}$ derivatives.[13,14] The total current produced by a representative photocell from initial irradiation until the photocurrent had decayed to a level commensurate with a bare TiO_2 film (∼4 h) corresponds to a turnover of 16 per dye molecule. Given that a single IrO_2 nanoparticle of 2 nm diameter has enough surface area to accommodate ∼15 chemisorbed dye molecules and only a few dye molecules are likely to coordinate both the IrO_2 and TiO_2 surfaces, these are lower limits for the quantum yields and turnover numbers of appropriately positioned molecules.

In conclusion, we have demonstrated an overall water splitting system that uses visible light to convert water to hydrogen and oxygen assisted by a small applied voltage. The low quantum efficiency is due to slow electron transfer from the $IrO_2 \cdot nH_2O$ nanoparticles to the oxidized dye. This reaction does not compete effectively with back electron transfer from TiO_2 to the dye. It should be possible to tune these rates by changing the distances between the ruthenium center and the oxide surfaces, as well as by changing the redox potentials of the sensitizing dye.

Acknowledgment. This work was supported by the U.S. Department of Energy, Office of Basic Energy Sciences, under grants DE-FG02-07ER15911 and DE-FG02-03ER15393. T.E.M. thanks Prof. James Hurst for helpful discussions about visible light water splitting.

Supporting Information Available: Synthesis and characterization of dye **1**, detailed experimental procedures, electron micrographs, UV−visible spectra, and transient absorbance data for dye-stabilized $IrO_2 \cdot nH_2O$ colloids. This material is available free of charge via the Internet at http://pubs.acs.org.

References

(1) Fujishima, A.; Honda, K. *Nature* **1972**, *238*, 37.
(2) Khaselev, O.; Turner, J. A. *Science* **1998**, *280*, 425.
(3) Licht, S.; Wang, B.; Mukerji, S.; Soga, T.; Umeo, M.; Tributsch, H. *Int. J. Hydrogen Energy* **2001**, *26*, 653.
(4) Maeda, K.; Teramura, K.; Lu, D.; Takata, T.; Sato, N.; Inoue, Y.; Domen, K. *Nature* **2006**, *440*, 295.
(5) Mandal, K.; Hoffman, M. Z. *J. Phys. Chem.* **1984**, *88*, 185.
(6) Harriman, A.; Richoux, M.; Christensen, P. A.; Moseri, S.; Neta, P. *J. Chem. Soc., Faraday Trans. 1* **1987**, *83*, 3001.
(7) Chen, H.; Faller, J. W.; Crabtree, R. H.; Brudvig, G. *J. Am. Chem. Soc.* **2004**, *126*, 7345.
(8) Zong, R.; Thummel, R. P. *J. Am. Chem. Soc.* **2005**, *127*, 12802.
(9) Kanan, M. W.; Nocera, D. G. *Science* **2008**, *321*, 1072.
(10) Concepcion, J. J.; Jurss, J. W.; Templeton, J. L.; Meyer, T. J. *Proc. Natl. Acad. Sci. U.S.A.* **2008**, *105*, 17632–17635.
(11) Brimblecombe, R.; Swiegers, G. F.; Dismukes, G. C.; Spiccia, L. *Angew. Chem.* **2008**, *47*, 7335.
(12) McDaniel, N. D.; Couglin, F. J.; Tinker, L. L.; Bernhard, S. *J. Am. Chem. Soc.* **2008**, *130*, 210.
(13) Harriman, A.; Pickering, I. J.; Thomas, J. M.; Christensen, P. A. *J. Chem. Soc., Faraday Trans. 1* **1988**, *84*, 2795.
(14) Morris, N. D.; Suzuki, M.; Mallouk, T. E. *J. Phys. Chem. A* **2004**, *108*, 9115.
(15) Hoertz, P. G.; Kim, Y. I.; Youngblood, W. J.; Mallouk, T. E. *J. Phys. Chem. B* **2007**, *111*, 6945.
(16) Gratzel, M. *Nature* **2001**, *414*, 338.

JA809108Y